

# Transmission Dynamics of Tuberculosis Model with Control Strategies

M. L. Olaosebikan, M. K. Kolawole, and K. A. Bashiru



Volume 4, Issue 2, Pages 110–118, December 2023

Received 10 July 2023, Revised 22 September 2023, Accepted 22 September 2023, Published Online 31 December 2023

To Cite this Article : M. L. Olaosebikan, M. K. Kolawole, and K. A. Bashiru, "Transmission Dynamics of Tuberculosis Model with Control Strategies", *Jambura J. Biomath*, vol. 4, no. 2, pp. 110–118, 2023, <https://doi.org/10.37905/jjbm.v4i2.21043>

© 2023 by author(s)

## JOURNAL INFO • JAMBURA JOURNAL OF BIOMATHEMATICS



	Homepage	:	<a href="http://ejurnal.ung.ac.id/index.php/JJBM/index">http://ejurnal.ung.ac.id/index.php/JJBM/index</a>
	Journal Abbreviation	:	Jambura J. Biomath.
	Frequency	:	Biannual (June and December)
	Publication Language	:	English (preferable), Indonesia
	DOI	:	<a href="https://doi.org/10.37905/jjbm">https://doi.org/10.37905/jjbm</a>
	Online ISSN	:	2723-0317
	Editor-in-Chief	:	Hasan S. Panigoro
	Publisher	:	Department of Mathematics, Universitas Negeri Gorontalo
	Country	:	Indonesia
	OAI Address	:	<a href="http://ejurnal.ung.ac.id/index.php/jjbm/oai">http://ejurnal.ung.ac.id/index.php/jjbm/oai</a>
	Google Scholar ID	:	XzYgeKQAAAAJ
	Email	:	<a href="mailto:editorial.jjbm@ung.ac.id">editorial.jjbm@ung.ac.id</a>

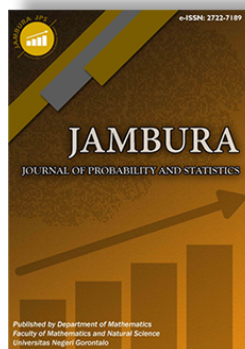
## JAMBURA JOURNAL • FIND OUR OTHER JOURNALS



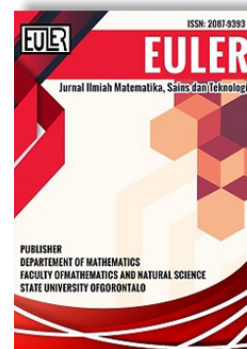
Jambura Journal of Mathematics



Jambura Journal of Mathematics Education



Jambura Journal of Probability and Statistics



EULER : Jurnal Ilmiah Matematika, Sains, dan Teknologi



# Transmission Dynamics of Tuberculosis Model with Control Strategies

M. L. Olaosebikan<sup>1,\*</sup> , M. K. Kolawole<sup>2</sup>, and K. A. Bashiru<sup>3</sup> 

<sup>1,2</sup>Department of Mathematical Sciences, Osun State University, Nigeria.

<sup>3</sup>Department of Statistics, Osun State University, Nigeria.

## ARTICLE HISTORY

Received 10 July 2023

Revised 22 September 2023

Accepted 22 September 2023

Published 31 December 2023

## KEYWORDS

mathematical model

tuberculosis

basic reproduction number

local stability

global stability

sensitivity analysis

python software

**ABSTRACT.** Tuberculosis (TB) is a global health concern, with a significant proportion of the population at severe risk of infection. Mathematical models can provide valuable insights into the transmission dynamics of TB, especially with the use of vaccination and the mixed proportional incidence rate. In this study, we developed a compartmental model to analyze the impact of mixing proportional incidence rates with vaccination on TB transmission. We conducted a qualitative study on the mathematical model, which included showing that it is unique, positively invariant, and bounded, showing that it is epidemiologically sound to study the physical transmission of TB. We used the homotopy perturbation method to obtain numerical solutions to the model. Using python software, we simulated the obtained results, and our results show that increasing vaccination coverage is an effective measure for reducing TB incidence. Furthermore, our analysis suggests that the mixing proportional incidence rate can be used to predict the spatial spread of TB in a population. It was concluded that vaccination and proportional incidence rate mixing are critical factors to be considered when developing effective TB control strategies.



This article is an open access article distributed under the terms and conditions of the Creative Commons Attribution-NonCommercial 4.0 International License. *Editorial of JJBM:* Department of Mathematics, Universitas Negeri Gorontalo, Jln. Prof. Dr. Ing. B. J. Habibie, Bone Bolango 96554, Indonesia.

## 1. Introduction

Tuberculosis (TB) is a contagious and deadly disease caused by the bacteria *Mycobacterium tuberculosis*. Despite the existence of the Bacillus Calmette-Guérin (BCG) vaccine and effective treatment options, TB continues to be a major global health threat, causing an estimated 1.4 million deaths annually [1–3]. One of the challenges in controlling TB is understanding how the disease spreads within a population and how vaccination can impact transmission dynamics. Mathematical modeling has been widely used to study the transmission of TB and has provided important insights into the effectiveness of various control strategies [4, 5]. In recent years, there has been significant research into the pathophysiology, diagnosis, and treatment of TB. This work has been documented in a wide range of literature, including scientific journals, textbooks, and other publications. Studies have focused on a variety of topics related to TB, such as the development of new diagnostic tools and treatment strategies, the role of host immune responses in disease progression, and the emergence of drug-resistant strains of the bacteria. This research has been critical in helping to improve our understanding of TB and in developing more effective approaches to preventing, diagnosing, and treating the disease [6, 7]. TB is primarily treated with antibiotics, but vaccination is also an important part of TB control efforts. The Bacille Calmette-Guérin (BCG) vaccine is the only vaccine currently available for preventing TB, and it is used widely in many parts of the world. Vaccination is a powerful tool for preventing and controlling infectious diseases [8–10]. It

works by stimulating the immune system to recognize and fight off specific pathogens, such as viruses or bacteria. Vaccination has been instrumental in the global control of many infectious diseases, such as smallpox, polio, and measles. The BCG vaccine has been in use for over 100 years, and while it is not fully protective against all forms of TB, it has been shown to be effective in reducing the risk of severe forms of the disease, such as TB meningitis and miliary TB, in children. BCG vaccination is recommended by the World Health Organization (WHO) for infants and children in countries with a high burden of TB. In addition to the BCG vaccine, there are ongoing efforts to develop new and more effective TB vaccines, with a particular focus on improving protection against pulmonary TB in adults. These efforts are part of a larger strategy to eliminate TB as a public health threat by 2030, as outlined in the WHO's End TB Strategy [2, 3, 11].

Mathematical models are often used to better understand how infectious diseases spread and how to prevent them [6, 12]. Many models on the dynamics of tuberculosis have been developed and examined to gain a better knowledge of the transmission dynamics and control of tuberculosis [4]. [13] developed a model to investigate the role of partial therapy in the transmission of tuberculosis disease. [14] examined a dynamical TB illness problem involving both hospitalized and non-hospitalized infectious classes. [2, 15] also presented a model for tuberculosis disease to estimate the impact of treatment and analysis for infectious individuals. The stability of tuberculosis with partial treatment is investigated by [11, 16]. investigated tuberculosis transmission by taking into account the existence of a latent group and vaccine administration to the susceptible class. The

\*Corresponding Author.

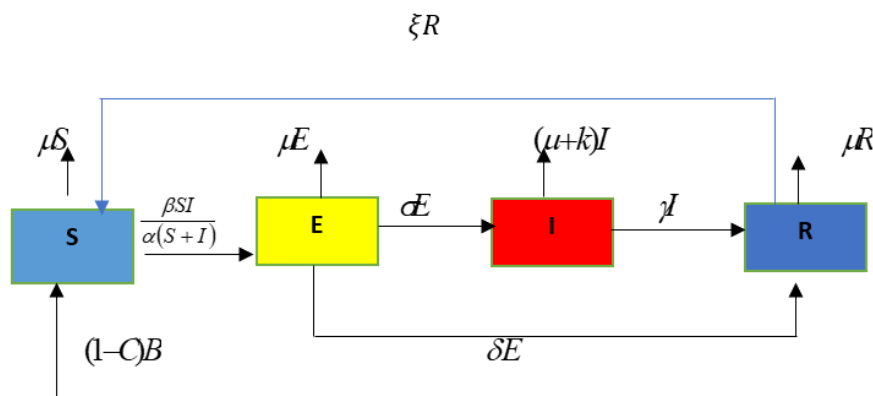


Figure 1. Schematic diagram of the model.

homotopy perturbation method (HPM), introduced by He (1999), is a powerful analytical tool used in solving nonlinear differential equations. HPM is a kind of perturbation method that involves the construction of a homotopy between a known linear problem and the original nonlinear problem and then applying perturbation theory to the homotopy parameter. HPM has been applied to a wide range of problems in various fields of science and engineering, including physics, chemistry, biology, and mathematics. To name a few, [17] extended the modified form of the method to solve fractional-order nonlinear integro-differential equations. Their results demonstrate the convergence and effectiveness of the method. Also, [12, 18] applied this same HPM to numerically simulate the effect of double-dose vaccination in their results, and they concluded that the method is a powerful tool that can be applied to study the trend of diseases through numerical simulations. Overall, the combination of HPM and numerical simulation provides a powerful tool for studying nonlinear problems and has been used in a wide range of applications, such as modeling physical systems, analyzing biological phenomena, and solving engineering problems. Other works on application of Homotopy Perturbation Method can be found in [16, 18–20]. As a motivation for this study, there is a need to alleviate the pressure on health care facilities in rural regions of developing countries such as Nigeria. As an alternative, we explore alternatives such as individual immunization and the proportional incidence rate of the masses. Consequently, we propose a modified mathematical model [21] to evaluate TB dynamics by including a vaccination parameter and mixing proportional incidence rates.

## 2. Methods

We develop a deterministic mathematical model on the transmission dynamics of tuberculosis based on the epidemiological status of individuals in the population. The population is subdivided into different epidemiological classes: susceptible ( $S$ ), exposed ( $E$ ), infected ( $I$ ) and recovered ( $R$ ) individuals. Recruitment into the susceptible population is at rate  $B$  and the force of infection is at a rate  $\beta$ , natural death rate occurs in all the classes at a rate  $\mu$ , the disease induced death rate for infected individuals is at a rate  $k$ . Individuals in the recovered class can become susceptible class after recovery at a rate  $\xi$ . The parameters  $C$  and  $\alpha$  represents the vaccination rate and saturated

term respectively. The above illustration can be represented in a schematic diagram and a system of nonlinear differential equations in Figure 1 and eq. (1) respectively.

$$\begin{aligned} \frac{dS}{dt} &= (1 - C)B - \frac{\beta SI}{\alpha(S + I)} - \mu S + \xi R \\ \frac{dE}{dt} &= \frac{\beta SI}{\alpha(S + I)} - a_1 E \\ \frac{dI}{dt} &= \sigma E - a_2 I \\ \frac{dR}{dt} &= \gamma I + \delta E + CB - a_3 R. \end{aligned} \tag{1}$$

where,

$$\begin{aligned} a_1 &= \delta + \mu + \sigma, \\ a_2 &= \gamma + \mu + k, \\ a_3 &= \xi + \mu, \end{aligned}$$

and the all parameters of eq. (1) can be seen in Table 1. As for the initial conditions of eq. (1) is given by

$$S(0) = s_0, E(0) = e_0, I(0) = i_0, R(0) = r_0 \geq 0. \tag{2}$$

## 3. Analysis of the model

### 3.1. Positivity and boundedness of solution

Consider the compartment of the system of equations for case (1) on the population, as obtained

$$N(t) = S(t) + E(t) + I(t) + R(t)$$

The variation in the total population with respect to time is given by:

$$\frac{dN(t)}{dt} = \frac{d}{dt} (S(t) + E(t) + I(t) + R(t)).$$

Such that

$$\frac{dN(t)}{dt} = B - \mu(S + E + I + R) - kI \Rightarrow \frac{dN(t)}{dt} \leq B - \mu N.$$

Thus, we have

$$\frac{dN(t)}{dt} + \mu N \leq B, \text{ leading to } N(t)e^{\mu t} = \frac{B}{\mu}e^{\mu t} + C. \tag{3}$$

**Table 1.** Description of parameters

Parameter	Definition
$C$	Vaccination Rate
$\sigma$	Progression rate from latent to infected
$k$	Disease induce death
$\alpha$	Saturated term
$B$	Recruitment rate
$\beta$	Contact rate
$\gamma$	Transmission rate from infected to recovery
$\mu$	Natural death rate
$\delta$	Transmission rate from exposed to recovery
$\xi$	Relapse

Initially,

$$N(0) = \frac{B}{\mu} + Ce^{-\mu(0)},$$

this yields

$$C = N(0) - \frac{B}{\mu}. \tag{4}$$

Thus, substituting eq. (4) into eq. (3) as time progressively increases yields:

$$\lim_{t \rightarrow \infty} N(t) \leq \lim_{t \rightarrow \infty} \left[ \frac{B}{\mu} + \left( N(0) - \frac{B}{\mu} \right) e^{-\mu t} \right] = \frac{B}{\mu}.$$

If  $N(0) \leq \frac{B}{\mu}$ , then  $N(t) \leq \frac{B}{\mu}$ . Thus  $D^\bullet$  is a positive invariant set under the flow described by eq. (2) so that no solution path leaves through any boundary of  $D^\bullet$ . Hence, it is sufficient to consider the dynamics of the model the domain  $D^\bullet$ . In this region the model can be considered has been mathematically and epidemiologically well posed.

This shows that the total population  $N(t)$ , the sub-population  $S(t), E(t), I(t), R(t)$  of the model are bounded and is a unique solution. Hence, its applicability to study physical system is feasible.

### 3.2. Existence and uniqueness of model solution

Let:

$$\begin{aligned} f_1 &= (1 - C)B - \frac{\beta SI}{\alpha(S + I) - \mu S + \xi R}, \\ f_2 &= \frac{\beta SI}{\alpha(S + I)} - a_1 E, \\ f_3 &= \sigma E - a_2 I, \\ f_4 &= \gamma I + \delta E + CB - a_3 R, \\ b &= \frac{\alpha\mu + \beta}{\alpha}. \end{aligned}$$

Then,

$$\begin{aligned} \left| \frac{df_1}{dS} \right| &= b, & \left| \frac{df_1}{dE} \right| &= 0, & \left| \frac{df_1}{dI} \right| &= \frac{\beta}{\alpha}, & \left| \frac{df_1}{dR} \right| &= \xi, \\ \left| \frac{df_2}{dS} \right| &= \frac{\beta}{\alpha}, & \left| \frac{df_2}{dE} \right| &= a_1, & \left| \frac{df_2}{dI} \right| &= \frac{\beta}{\alpha}, & \left| \frac{df_2}{dR} \right| &= 0, \\ \left| \frac{df_3}{dS} \right| &= 0, & \left| \frac{df_3}{dE} \right| &= \sigma, & \left| \frac{df_3}{dI} \right| &= a_2, & \left| \frac{df_3}{dR} \right| &= 0, \\ \left| \frac{df_4}{dS} \right| &= 0, & \left| \frac{df_4}{dE} \right| &= \delta, & \left| \frac{df_4}{dI} \right| &= \gamma, & \left| \frac{df_4}{dR} \right| &= a_3 < \infty, \end{aligned}$$

The solution of the model is bounded, well-posed and epidemiologically and mathematical represented.

### 3.3. Existence of disease free equilibrium state

At disease free equilibrium point, there is no outbreak of disease. Thus  $E = I = 0$  in system eq. (1). To get the disease free equilibrium point, first we set

$$\frac{dS}{dt} = \frac{dE}{dt} = \frac{dI}{dt} = \frac{dR}{dt} = 0. \tag{5}$$

From eq. (5) we have

$$(1 - C)B - \frac{\beta SI}{\alpha(S + I)} - \mu S + \xi R = 0, \tag{6}$$

$$\frac{\beta SI}{\alpha(S + I)} - a_1 E = 0, \tag{7}$$

$$\sigma E - a_2 I = 0, \tag{8}$$

$$\gamma I + \delta E + CB - a_3 R = 0. \tag{9}$$

Let  $I = 0, S_o \neq 0$ , from eq. (8),

$$\begin{aligned} \sigma E &= 0, \\ E &= 0. \end{aligned}$$

Next, for eq. (9), we get

$$\begin{aligned} CB - a_3 R &= 0, \\ \frac{CB}{a_3} &= R. \end{aligned}$$

Lastly, from eq. (6) we obtain,

$$\begin{aligned} (1 - C)B - \mu S + \xi R &= 0, \\ \xi R + (1 - C)B &= \mu S, \\ \frac{B[a_3(1 - C)]}{\mu a_3} &= S. \end{aligned}$$

Thus, the disease free equilibrium yields:

$$E_o = \left( \frac{B[a_3(1 - C)]}{\mu a_3}, 0, 0, \frac{CB}{a_3} \right).$$

**Table 2.** Values of model's parameter and references

Parameters	Definitions	Values	References
$C$	Vaccination Rate	0.108	[15]
$\sigma$	Progression rate from Latent to infected	0.00375	Assumed
$k$	Disease induce death	0.1	[11]
$\alpha$	Saturated term	0.1	Assumed
$B$	Recruitment rate	5	Assumed
$\beta$	Contact rate	0.6501	[11]
$\gamma$	Transmission rate from infected to recovery	0.05	Assumed
$\mu$	Natural death rate	$\frac{1}{67.7}$	[11]
$\delta$	Transmission rate from expose to recovery	0.1	Assumed
$\xi$	Relapse	0.5	Assumed

**3.4. Endemic equilibrium point**

Let  $E_e = (S^*, E^*, I^*, R^*)$  as Endemic Equilibrium where  $I \neq 0$ . Consider the system of eq. (1) the equilibrium points are:

$$S^* = \frac{a_2 a_3 [B(1 - C) + a_2 E^*] + \xi [E^* (a_2 \sigma \gamma + \delta) + CB]}{\mu a_2 a_3},$$

$$E^* = \frac{\beta S^* I^*}{\alpha a_1 (S^* + I^*)},$$

$$I^* = \frac{\sigma E^*}{a_2},$$

$$R^* = \frac{(a_2 \sigma \gamma + \delta) E^* + CB}{a_2 a_3}$$

**3.5. Basic reproduction number**

The system of eq. (1) contains two disease states, where only one state leads to new infections. The relationship between the Exposed, Infected compartments in eq. (1) depicts the number of secondary infections generated by infected individuals within the population. The basic reproductive ratio is determined by employing the next generation matrix. It is given by:

$$R_0 = \rho(|G - \lambda I|),$$

where  $G = F \times V^{-1}$  and  $\rho$  is the spectral radius of matrix  $|G - \lambda I|$ . Hence, calculating the  $R_0$  we used

$$\frac{dE}{dt} = \frac{\beta SI}{\alpha(S + I)} - a_1 E, \tag{10}$$

$$\frac{dI}{dt} = \sigma E - a_2 I. \tag{11}$$

From the system of eqs. (10) and (11) we obtained matrix  $F$  is

$$F_i = \left[ \frac{\partial f_i(x_i)}{\partial x_j} \right],$$

$$F^* = \begin{bmatrix} \frac{\beta}{\alpha} \\ 0 \end{bmatrix},$$

and matrix  $V$  is

$$V_i = \left[ \frac{\partial v_i(x_i)}{\partial x_j} \right],$$

$$V^* = \begin{bmatrix} a_1 E \\ -\sigma E + a_2 I \end{bmatrix}.$$

Thus;

$$F = \begin{bmatrix} \frac{\beta}{\alpha} & 0 \\ 0 & 0 \end{bmatrix}, V = \begin{bmatrix} a_1 & 0 \\ -\sigma & a_2 \end{bmatrix}.$$

Hence,

$$V^{-1} = \begin{bmatrix} \frac{1}{a_1} & \frac{\sigma}{a_1 a_2} \\ 0 & \frac{1}{a_2} \end{bmatrix}.$$

Thus, the  $R_0$  is obtained as

$$R_0 = \frac{\sigma \beta}{\alpha a_1 a_2}.$$

**3.6. Local stability of disease free equilibrium**

The disease free equilibrium (DFE) of the proposed epidemic model is locally asymptotically stable if  $R_0 < 1$  and unstable if  $R_0 > 1$ . The disease free equilibrium is obtained as

$$E_o = \left( \frac{B [a_3 (1 - C)]}{\mu a_3}, 0, 0, \frac{CB}{a_3} \right).$$

The Jacobian matrix of the system of eq. (1) is obtained and evaluated at the disease free state using linearization method

$$J_{(E_o)} = \begin{vmatrix} -\left[ \frac{\mu \alpha (1+I) + \beta I}{\alpha (1+I)} \right] & 0 & \frac{\beta S}{\alpha (S+1)} & \xi \\ \frac{\beta I}{\alpha (1+I)} & -a_1 & 0 & 0 \\ 0 & \sigma & -a_2 & 0 \\ 0 & \delta & \gamma & -a_3 \end{vmatrix},$$

for the eigenvalues,  $|J_{E_1} - \lambda_i I| = 0$

$$\begin{vmatrix} -\mu - \lambda_1 & 0 & \frac{\beta S_o}{\alpha (S_o+1)} & \xi \\ 0 & -a_1 - \lambda_2 & 0 & 0 \\ 0 & \alpha & -a_2 - \lambda_3 & 0 \\ 0 & \delta & \gamma & -a_3 - \lambda_4 \end{vmatrix} = 0,$$

and we obtain:

$$\lambda_1 = -\mu,$$

$$\lambda_2 = -a_1,$$

$$\lambda_3 = -a_2,$$

$$\lambda_4 = -a_3.$$

The eigenvalues are negative, hence the system of eq. (1) is stable.

**3.7. Local stability of endemic equilibrium**

The endemic equilibrium of the proposed epidemic model is locally asymptotically stable if  $R_0 > 1$  and unstable otherwise.

Let

$$\begin{aligned} S &= p + S^*, \\ E &= q + E^*, \\ I &= x + I^*, \\ R &= y + R^*. \end{aligned}$$

Linearizing eq. (1), eq. (12) is then obtained as:

$$\begin{aligned} \frac{dp}{dt} &= -\beta xp\alpha (x+p)^{-1} - \mu p + \xi y + O, \\ \frac{dq}{dt} &= \beta xp\alpha (x+p)^{-1} - a_1 q + O, \\ \frac{dx}{dt} &= \sigma q - a_2 x + O, \\ \frac{dy}{dt} &= \gamma x + \delta q + \beta c - a_3 y + O, \end{aligned} \tag{12}$$

where

$$O = \text{Higher order} + \text{nonlinear terms} \dots$$

Thus, the Jacobian matrix of the system of eq. (12),

$$J_{(E_e)} = \begin{pmatrix} -\left[\frac{\beta x\alpha + \mu(x+1)}{(x+1)}\right] & 0 & -\frac{\beta p\alpha}{(p+1)} & \xi \\ \frac{\beta x\alpha}{(x+1)} & -a_1 & 0 & 0 \\ 0 & \sigma & -a_2 & 0 \\ 0 & \delta & \gamma & -a_3 \end{pmatrix},$$

The resulting eigenvalue of the above matrix is obtained as

$$(A_1 - \lambda_1)(A_2 - \lambda_2)(A_3 - \lambda_3)(A_4 - \lambda_4) = 0, \tag{13}$$

where

$$\begin{aligned} A_1 &= -\left[\frac{\beta x\alpha + \mu(x+1)}{(x+1)}\right], \\ A_2 &= -a_1, \\ A_3 &= -a_2, \\ A_4 &= -a_3. \end{aligned}$$

From eq. (13) we get characteristic equation

$$\lambda^4 - Z_1\lambda^3 + Z_2\lambda^2 - Z_3 + Z_4,$$

with

$$\begin{aligned} Z_1 &= A_1 + A_2 + A_3 + A_4, \\ Z_2 &= (A_1 + A_2)(A_3 + A_4) + A_1A_2 + A_3A_4, \\ Z_3 &= A_1A_2(A_3 + A_4) + A_3A_4(A_1 + A_2), \\ Z_4 &= A_1A_2A_3A_4. \end{aligned}$$

Therefore, they are locally asymptotically stable.

### 3.8. Global stability of disease free equilibrium

Using Lyapunov function approach to proceed for the result for global asymptotic stability of the proposed system of eq. (1), at disease free equilibrium state. Using Lyapunov algorithm;

$$M(S, E, I, R, t) = W_1I_1 + W_2I_2.$$

we have

$$\begin{aligned} M^* &= W_1I_1^* + W_2I_2^*, \\ &= W_1 \left( \frac{\beta SI}{\alpha(S+I)} - a_1E \right) + W_2 (\sigma E - a_2I), \\ &= W_1 \left( \frac{\beta S_0}{\alpha} - a_1I_1 \right) + W_2 (\sigma I_1 - a_2I_2), \\ &= W_1 \frac{\beta S_0}{\alpha} - a_1W_1I_1 + W_2\sigma I_1 - a_2W_2I_2, \\ &\leq [W_2\sigma - a_1W_1] I_1 + \left[ W_1 \frac{\beta S_0}{\alpha} - a_2W_2 \right] I_2, \end{aligned}$$

with  $M^* = \frac{dM}{dt}$  and  $S_0 = \frac{B[a_3(1-C)]}{\mu a_3}$ . Then, let  $W_1 = \frac{1}{a_1}$  and  $W_2 = \frac{\beta B[a_3(1-C)]}{\alpha \mu a_1 a_2 a_3}$ , we get

$$\begin{aligned} M^* &\leq \left[ \frac{\beta B [a_3 (1 - C)]}{\alpha \mu a_1 a_2 a_3} - 1 \right] I_1, \\ &\leq \mu_0 [R_0 - 1] I. \end{aligned}$$

It is imperative to note that  $M^* = 0$  when  $I = 0$ . Thus, substituting  $I = 0$  into the system of eq. (1) shows that  $S_0 = \frac{B[a_3(1-C)]}{\mu a_3}$  at  $t \rightarrow \infty$ ,  $C < 1$ ,  $\mu_0 = \frac{\mu}{B[a_3(1-C)]}$ . Based on LaSalle's invariance principle. Hence  $E_0 = 0$  is globally asymptotically stable whenever  $R_0 < 1$ .

### 3.9. Sensitivity analysis of $R_0$

Table 3. Parameter and indices of sensitivity analysis

Parameter	Sensitivity
$\beta$	1.000000
$k$	2.5438996911
$\sigma$	1.0326737
$\gamma$	0.5492368266
$\mu$	-0.02150145349
$\delta$	1.000000
$\alpha$	-1.000000

Our objective is to evaluate the sensitivity of  $R_0$  by taking its derivative with respect to all its parameters. The normalized forward sensitivity index is denoted as;

$$\begin{aligned} \frac{\partial R_0}{\partial \beta} &= \frac{\partial R_0}{\partial \beta} \times \frac{\beta}{R_0} = 1.000000, \\ \frac{\partial R_0}{\partial \sigma} &= \frac{\partial R_0}{\partial \sigma} \times \frac{\sigma}{R_0} = 1.0326737, \\ \frac{\partial R_0}{\partial \alpha} &= \frac{\partial R_0}{\partial \alpha} \times \frac{\alpha}{R_0} = 0.1, \\ \frac{\partial R_0}{\partial \mu} &= \frac{\partial R_0}{\partial \mu} \times \frac{\mu}{R_0} = 0.1853567228, \\ \frac{\partial R_0}{\partial k} &= \frac{\partial R_0}{\partial k} \times \frac{k}{R_0} = 2.5438996911, \\ \frac{\partial R_0}{\partial \delta} &= \frac{\partial R_0}{\partial \delta} \times \frac{\delta}{R_0} = 1.000000, \\ \frac{\partial R_0}{\partial \gamma} &= \frac{\partial R_0}{\partial \gamma} \times \frac{\gamma}{R_0} = 0.5492368266. \end{aligned}$$

Table 3, shows that the sensitivity indices of  $\beta, \sigma, \gamma$  are positive, while those of the other parameters are negative. As the sensitivity indices depend on the values of the other parameters, changes in those values will affect the sensitivity indices. Based on the table, we can conclude that parameters  $\beta$  and  $\sigma$  are the most sensitive to the basic reproduction number  $R_0$  in eq. (1) of the tuberculosis model. Specifically, increasing the value of  $\sigma$  will result in a 99.96% increase in  $R_0$ , while increasing the value of  $\delta$  will lead to a 98.62% decrease in  $R_0$ .

### 4. Numerical solution of the model with Homotopy perturbation method

Since we intend to numerically simulate the mathematical model, we intend to provide an approximate solution using the

homotopy perturbation method since there is no associated exact solution to the model. The analysis of the HPM will be given

$$\Delta(\alpha) = k(\tau), \quad \tau \in \lambda.$$

Subject to the boundary condition

$$\Psi(\alpha, \alpha_n) = 0 \quad \tau \in \Pi. \tag{14}$$

Operator  $\Delta$  represents the differential operator,  $\Psi$  denotes the boundary operator,  $k(\tau)$  is an analytic function,  $\Phi$  is a defined domain bounded by  $\Pi$ , and  $\alpha_n$  is a normal vector derivative drawn externally from  $\Phi$ . Thus we can separate the operator  $\Delta(\alpha)$  into two:

$$\Delta(\alpha) = L_T(\alpha) + N_T(\alpha),$$

The operator  $L_T(\alpha), N_T(\alpha)$  denotes the linear and nonlinear term respectively such that eq. (14) implies:

$$L_T(\alpha) + N_T(\alpha) = k(\tau), \quad \tau \in \lambda.$$

We can construct a Homotopy for eq. (15) so that

$$H(f, p) = (1 - p) [L_T(f) - L_T(\omega_0)] + p [\Delta(f) - k(r)] = 0, \tag{15}$$

where  $p$  is an embedding parameter which can undergo a deformation process of changing from  $[0, 1]$ . Equation (16) is further simplified to obtain:

$$H(f, p) = L_T(f) - L_T(\alpha_0) + p[L_T(\alpha_0)] + p[N_T(\alpha_0) - k(\tau)] = 0, \tag{16}$$

as  $p \rightarrow 0$ , eq. (17) yields:

$$H(f, 0) = L_T(f) - L_T(\alpha_0) = 0, \tag{17}$$

and when  $p \rightarrow 1$ ,

$$H(f, 1) = \Delta(f) - k(\tau) = 0.$$

We can naturally assume the solution eq. (18) as a power series such that

$$f(t) = f_0(t) + pf_1(t) + p^2f_2(t) + \dots + p^n f_n(t) \tag{18}$$

Evaluating eq. (18) with eq. (19), and comparing coefficients of equal powers of  $p$ . The values of  $f_0(t), f_1(t), f_2(t)$  are obtained by solving the resulting ordinary differential equations. Thus, the approximate solution of eq. (17) is:

$$f(t) = \lim_{p \rightarrow 1} f_n(t) = f_0(t) + f_1(t) + f_2(t) + \dots \tag{19}$$

To conduct numerical simulation on the mathematical model, we create the following correctional scheme for the model equation.

$$(1 - p) \frac{dS}{dt} + p \left( \frac{dS}{dt} - (1 - C)B + \frac{\beta SI}{\alpha(S + I)} + \mu S - \xi R \right) = 0,$$

$$(1 - p) \frac{dE}{dt} + p \left( \frac{dE}{dt} - \frac{\beta SI}{\alpha(S + I)} + a_1 E \right) = 0,$$

$$(1 - p) \frac{dI}{dt} + p \left( \frac{dI}{dt} - \sigma E + a_2 I \right) = 0,$$

$$(1 - p) \frac{dR}{dt} + p \left( \frac{dR}{dt} - \gamma I - \delta E - CB + a_3 R \right).$$

Simplifying the preceding equation yields:

$$\begin{aligned} \frac{dS}{dt} &= p \left( (1 - C)B - \frac{\beta SI}{\alpha(S + I)} - \mu S + \xi R \right) \\ \frac{dE}{dt} &= p \left( \frac{\beta SI}{\alpha(S + I)} - a_1 E \right) \\ \frac{dI}{dt} &= p (\sigma E - a_2 I) \\ \frac{dR}{dt} &= p (\gamma I + \delta E + CB - a_3 R) \end{aligned} \tag{20}$$

The approximate solution of eq. (1) can be assumed as:

$$\begin{aligned} S(t) &= s_0(t) + ps_1(t) + p^2s_2(t) + \dots + p^n s_n(t) \\ E(t) &= e_0(t) + pe_1(t) + p^2e_2(t) + \dots + p^n e_n(t) \\ I(t) &= i_0(t) + pi_1(t) + p^2i_2(t) + \dots + p^n i_n(t) \\ R(t) &= r_0(t) + pr_1(t) + p^2r_2(t) + \dots + p^n r_n(t) \end{aligned} \tag{21}$$

Evaluating eq. (20) using eq. (21) and comparing coefficient of  $p^n$ ,

$$p^0 : \dot{i}_0(t) = 0, \dot{e}_0(t) = 0, \dot{i}_0(t) = 0, \dot{r}_0(t) = 0,$$

we have that

$$s_0(t) = s_0, e_0(t) = e_0, i_0(t) = i_0, r_0(t) = r_0.$$

Similarly comparing the coefficients of  $p^1$ ,

$$\begin{aligned} \frac{ds_1}{dt} &= (1 - C)B - \frac{\beta s_0 i_0}{\alpha(s_0 + i_0)} - \mu s_0 + \xi r_0 \\ \frac{de_1}{dt} &= \frac{\beta s_0 i_0}{\alpha(s_0 + i_0)} - a_1 e_0 \\ \frac{di_1}{dt} &= \sigma e_0 - a_2 i_0 \\ \frac{dr_1}{dt} &= \gamma i_0 + \delta e_0 + CB - a_3 r_0 \end{aligned}$$

Solving the system yields:

$$\begin{aligned} s_1(t) &= \left( (1 - C)B - \frac{\beta s_0 i_0}{\alpha(s_0 + i_0)} - \mu s_0 + \xi r_0 \right) t \\ e_1(t) &= \left( \frac{\beta s_0 i_0}{\alpha(s_0 + i_0)} - a_1 e_0 \right) t \\ i_1(t) &= (\sigma e_0 - a_2 i_0) t \\ r_1(t) &= (\gamma i_0 + \delta e_0 + CB - a_3 r_0) t \end{aligned}$$

Following the iterative scheme, two more iterations are computed and the approximate results are evaluated, such that:

$$\begin{aligned} S(t) &= \sum_{n=0}^4 s_n(t), \\ E(t) &= \sum_{n=0}^4 e_n(t), \\ I(t) &= \sum_{n=0}^4 i_n(t), \\ R(t) &= \sum_{n=0}^4 r_n(t). \end{aligned}$$

The approximate results of each class are evaluated using their respective baseline values on Table 2. We also suggest the following population data set as initial values given by

$$s_0 = 1000, e_0 = 30, i_0 = 20, r_0 = 40.$$

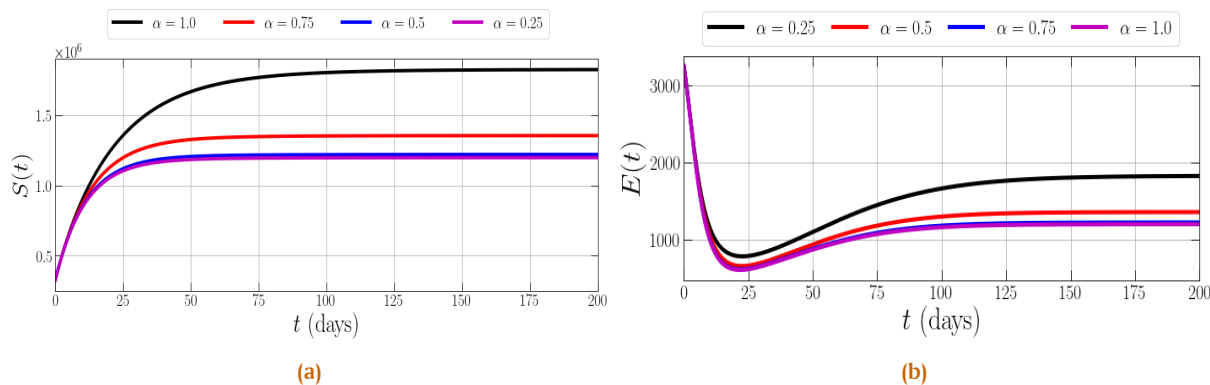


Figure 2. Dynamical behavior of susceptible and exposed population to  $\alpha$ .

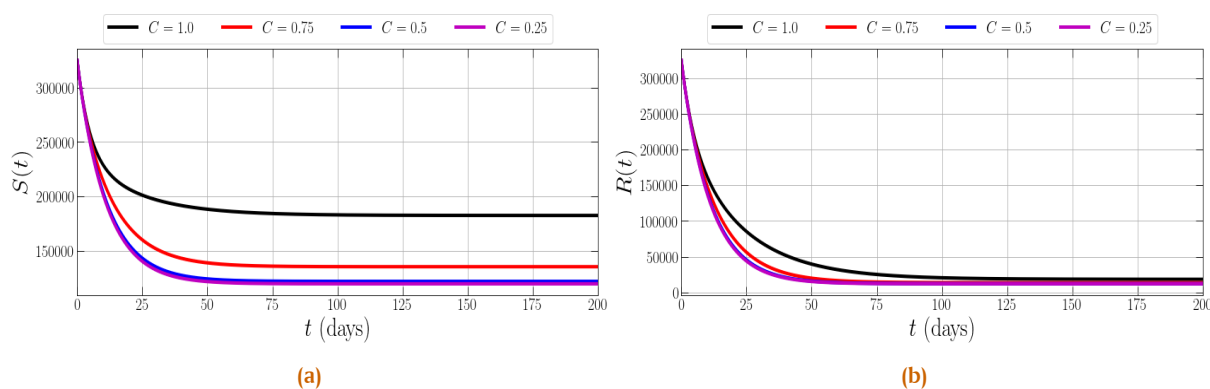


Figure 3. Impact of vaccination  $C$  on susceptible and recovered population.

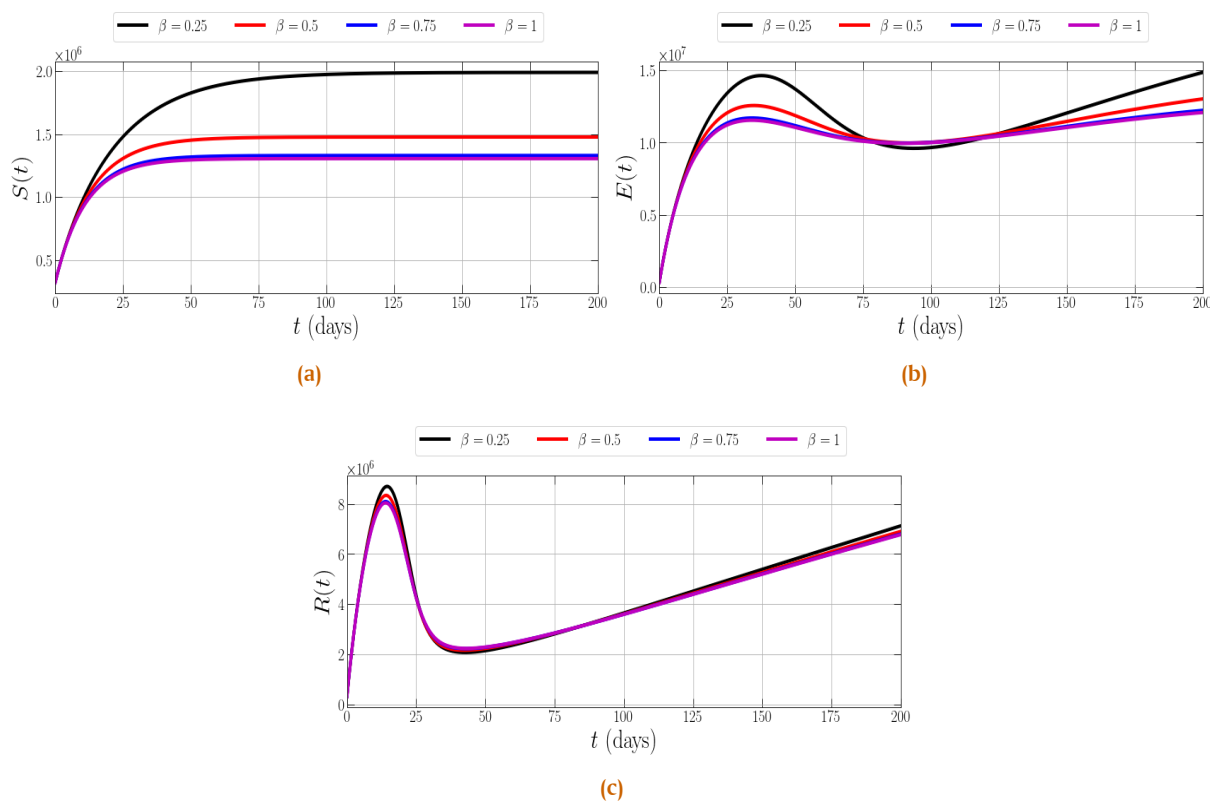


Figure 4. Effects of contact rate  $\beta$  on susceptible, exposed, and recovered population.



**Table 4.** Values of eq. (22)

Parameter	value	Parameter	value	Parameter	value	Parameter	value
$j_1$	1000	$j_{21}$	302.0838612	$j_{41}$	1164.133657	$j_{61}$	$2.468040000 \cdot 10^{-8}$
$j_2$	65.26869000	$j_{22}$	36988.74452	$j_{42}$	0.7679873978	$j_{62}$	0.004330716805
$j_3$	1.3362000	$j_{23}$	84.74264814	$j_{43}$	1431.639314	$j_{63}$	40
$j_4$	1362.924000	$j_{24}$	30	$j_{44}$	1.875838588	$j_{64}$	46.18360
$j_5$	37.68	$j_{25}$	45.62599000	$j_{45}$	16753.17626	$j_{65}$	37.68
$j_6$	8.99856418	$j_{26}$	1362.924999	$j_{46}$	0.0003841080404	$j_{66}$	250.8099123
$j_7$	5499.838828	$j_{27}$	1.336200000	$j_{47}$	16.31203298	$j_{67}$	45.9850488
$j_8$	54.0914019	$j_{28}$	69.38980854	$j_{48}$	36988.74452	$j_{68}$	2044.386000
$j_9$	152.0510083	$j_{29}$	8.998569418	$j_{49}$	84.74264814	$j_{69}$	2.004300000
$j_{10}$	0.09970881600	$j_{30}$	5499.839928	$j_{50}$	20	$j_{70}$	13.49785413
$j_{11}$	3333.926349	$j_{31}$	152.0510083	$j_{51}$	50.40320	$j_{71}$	8249.759899
$j_{12}$	45.98509816	$j_{32}$	0.09970881600	$j_{52}$	127.0391180	$j_{72}$	727.7734324
$j_{13}$	3.288025569	$j_{33}$	5378.993811	$j_{53}$	0.681642000	$j_{73}$	228.0765125
$j_{14}$	11.30828286	$j_{34}$	0.0000493608	$j_{54}$	0.000668100	$j_{74}$	0.1495632240
$j_{15}$	66.76103861	$j_{35}$	5.292993669	$j_{55}$	0.004499284709	$j_{75}$	10561.77617
$j_{16}$	0.003719829888	$j_{36}$	11.30828286	$j_{56}$	320.2194878	$j_{76}$	56.12053936
$j_{17}$	40645.08576	$j_{37}$	80.26339203	$j_{57}$	2.749919964	$j_{77}$	10.38388802
$j_{18}$	935.98111186	$j_{38}$	105.5276927	$j_{58}$	0.07602550416		
$j_{19}$	56.12092345	$j_{39}$	0.003719829888	$j_{59}$	0.00004985440800		
$j_{20}$	5.923814565	$j_{40}$	48897.59557	$j_{60}$	4.407401276		

Thus, we obtain the following series results embedding the parameters whose influence on the dynamics of tuberculosis transmission are to be analyzed.

where the values of parameters  $j_1$  to  $j_{77}$  in eq. (22) can be seen in Table 4.

### 5. Results and Discussion

Here Python software was used to simulate the dynamics of the disease at a progressing time. The results are graphically presented and extensively discussed:

#### 5.1. Discussion of results

The vulnerable population increases as the saturated term increases. Figure 2a shows that as  $\alpha$  increases from 0.25 to 1, the susceptible population increase. The implication of this is that, increase in saturation term will increase the population of the susceptible while decrease, in saturation term will decrease the population of the susceptible. As the rate of saturation increases, exposed population decreases. It was observed from Figure 2b that when  $\alpha$  increases from 0.25 to 1.0, the Exposed population is also decreasing, at time (days) over a period of 200 days. Figure 3a show that increase in vaccination will reduced the number of infected individuals, and this will lead to an increase in the population of the susceptible individuals. Figure 3b show the impact of vaccination  $C$  on recovered population, upon recovery, recovered individuals through treatment can be susceptible to the disease again. In this case, vaccination of recovered individuals will drastically reduce the disease epidemic in the population. Figure 4a and 4b show the effects of contact rate  $\beta$  on susceptible and exposed population respectively. It is shown that, increasing contact rate will reduce the population of the susceptible individuals this is seen when  $\beta$  is 1, in this case more people will be infected thereby increasing the population of the infected individuals, subsequently reducing it will increase the susceptible population. Figure 4c show the effects of contact rate  $\beta$  on recovered population, Increasing contact rate will reduce the population of the recovered individuals. In this case more people will be infected thereby increasing the population of the infected individuals, subsequently reducing it will increase the susceptible population.

$$\begin{aligned}
 s(t) &= j_1 + \begin{pmatrix} j_2 + j_3\alpha \\ -j_4\alpha^2 - j_5c \end{pmatrix} t + \begin{pmatrix} -j_6\alpha^2 \\ +j_7\alpha^4 \\ j_8 \\ +j_9\alpha^2c \\ -j_{10}\alpha c \\ +j_{11} \\ j_{12}c \\ -j_{13}\alpha \end{pmatrix} \frac{t^2}{2} - \begin{pmatrix} j_{14}\alpha^2c^2 \\ -j_{15}\alpha^3 \\ -j_{16}\alpha c^2 \\ +j_{17}\alpha^4 \\ +j_{18}\alpha^2c \\ +j_{19}c \\ -j_{20}\alpha \\ j_{21} \\ +j_{22}\alpha^6 \\ -j_{23}\alpha \end{pmatrix} \frac{t^3}{6}, \\
 e(t) &= j_{24} + \begin{pmatrix} -j_{25} \\ +j_{26}\alpha^2 \\ -j_{27}\alpha \end{pmatrix} t - \begin{pmatrix} -j_{28} \\ -j_{29}\alpha^3 \\ +j_{30}\alpha^4 \\ +j_{31}\alpha^2c \\ -j_{32}\alpha c \\ +j_{33}\alpha^2 \\ +j_{34}c \\ -j_{35}\alpha \end{pmatrix} \frac{t^2}{2} + \begin{pmatrix} j_{36}\alpha^2 - j_{37}\alpha^3 \\ -j_{38} - j_{39}\alpha c \\ +j_{40}\alpha^4 + j_{41}\alpha^2c \\ -j_{42}\alpha c + j_{43}\alpha^4c \\ -j_{44}\alpha^3c + j_{45}\alpha^2 \\ +j_{46}c - j_{47}\alpha \\ +j_{48}\alpha^6 - j_{49}\alpha^5 \end{pmatrix} \frac{t^3}{6}, \\
 i(t) &= j_{50} - j_{51}t - \begin{pmatrix} j_{52} \\ +j_{53}\alpha^2 \\ -j_{54}\alpha \end{pmatrix} \frac{t^2}{2} - \begin{pmatrix} -j_{55}\alpha^3 \\ +j_{56} \\ +j_{57}\alpha^4 \\ +j_{58}\alpha^2c \\ -j_{59}\alpha c \\ +j_{60}\alpha^2 \\ +j_{61}c \\ -j_{62}\alpha \end{pmatrix} \frac{t^3}{6}, \\
 r(t) &= j_{63} + (j_{64} + j_{65}t) - \begin{pmatrix} j_{66} \\ +j_{67}c \\ -j_{68}\alpha^2 \\ +j_{69}\alpha \end{pmatrix} \frac{t^2}{2} + \begin{pmatrix} j_{70}\alpha^3 \\ -j_{71}\alpha^4 \\ +j_{72} \\ -j_{73}\alpha^2c \\ +j_{74}\alpha c \\ -j_{75}\alpha^2 \\ +j_{76}c \\ +j_{77}\alpha \end{pmatrix} \frac{t^3}{6},
 \end{aligned}
 \tag{22}$$

## 6. Conclusion

In this paper, a modified dynamic model is introduced to examine the impact of mixing proportional incidence rate on the transmission of tuberculosis. Through analysis of the model, it is demonstrated that a strategy incorporating both elevated vaccination rates and monitoring of actual TB spread could effectively eradicate tuberculosis from our society. The analysis suggests that the mixing proportional incidence rate can be used to predict the spatial spread of TB in a population. It was concluded that vaccination and proportional incidence rate mixing are critical factors to consider when developing effective TB control strategies.

**Author Contributions.** Olaosebikan, M.L.: Conceptualization, methodology, software, validation, project administration, funding acquisition. Kolawole, M.K.: Writing—review and editing, visualization, supervision, project administration. Bashiru, K.A.: Validation, formal analysis, investigation.

**Acknowledgement.** The authors are thankful the editors and reviewers who have supported us in improving this manuscript.

**Funding.** None.

**Conflict of interest.** The authors declare no conflict of interest.

**Data availability.** Not applicable.

## References

- [1] B. M. Murphy, B. H. Singer, and D. Kirschner, "On treatment of tuberculosis in heterogeneous populations," *Journal of Theoretical Biology*, vol. 223, no. 4, pp. 391–404, 2003. DOI:10.1016/S0022-5193(03)00038-9
- [2] T. M. Daniel, J. H. Bates, and K. A. Downes, *History of Tuberculosis*. John Wiley & Sons, Ltd, 1994, ch. 2, pp. 13–24. ISBN 9781683672753. DOI:10.1128/9781555818357.ch2
- [3] W. H. Organization *et al.*, "World health organization global tuberculosis report 2021," URL: <https://www.who.int/teams/global-tuberculosis-programme/tbreports/global-tuberculosis-report-2021>, Accessed on 14 October 2021.
- [4] K. A. Bashiru, O. Fasoranbaku, T. Ojurongbe, M. Lawal, A. Abiona, and B. Oluwasanmi, "A Stochastic Model to Analyze and Predict Transmission Dynamics of Tuberculosis in Ede Kingdom of Osun State," *Fountain Journal of Natural and Applied Sciences*, vol. 7, no. 1, pp. 12–19, 2018. DOI:10.53704/fujnas.v7i1.182
- [5] S. Khajanchi, D. K. Das, and T. K. Kar, "Dynamics of tuberculosis transmission with exogenous reinfections and endogenous reactivation," *Physica A: Statistical Mechanics and its Applications*, vol. 497, pp. 52–71, 2018. DOI:10.1016/j.physa.2018.01.014
- [6] S. Bisuta, P. Kayembe, M. Katedi, H. Situakibanza, J. Ditekemena, A. Bakebe, G. Lay, G. Mesia, J. Kayembe, and S. Fueza, "Trends of bacteriologically confirmed pulmonary tuberculosis and treatment outcomes in democratic republic of the congo: 2007–2017," *Ann. Afr. Med.*, vol. 11, no. 4, pp. 2974–2985, 2018.
- [7] M. Dauda, A. Magaji, P. Okolo, J. Bulus, and U. Shehu, "Analyzing the transmission dynamics of tuberculosis in kaduna metropolis, nigeria," *Science World Journal*, vol. 15, no. 4, pp. 76–82, 2020.
- [8] F. Firmansyah and Y. M. Rangkuti, "Sensitivity Analysis and Optimal Control of Covid 19 Model," *Jambura Journal of Biomathematics (JJBM)*, vol. 4, no. 1, pp. 95–102, 2023. DOI:10.34312/jjbm.v4i1.19025
- [9] M. Manaqib, M. Mahmudi, and G. Prayoga, "Mathematical Model and Simulation of the Spread of COVID-19 with Vaccination, Implementation of Health Protocols, and Treatment," *Jambura Journal of Biomathematics (JJBM)*, vol. 4, no. 1, pp. 69–79, 2023. DOI:10.34312/jjbm.v4i1.19162
- [10] R. Resmawan, L. Yahya, R. S. Pakaya, H. S. Panigoro, and A. R. Nuha, "Analisis Dinamik Model Penyebaran COVID-19 dengan Vaksinasi," *Jambura Journal of Biomathematics (JJBM)*, vol. 3, no. 1, 2022. DOI:10.34312/jjbm.v3i1.13176
- [11] Fatmawati, M. A. Khan, C. Alfiniyah, and E. Alzahrani, "Analysis of dengue model with fractal-fractional Caputo–Fabrizio operator," *Advances in Difference Equations*, vol. 2020, no. 1, pp. 1–23, 2020. DOI:10.1186/s13662-020-02881-w
- [12] T. A. Ayoola, M. K. Kolawole, and A. O. Popoola, "Mathematical model of covid-19 transmission dynamics with double dose vaccination," *Tanzania Journal of Science*, vol. 48, no. 2, pp. 499–512, 2022. DOI:10.4314/tjs.v48i2.23
- [13] Y. Yang, J. Li, Z. Ma, and L. Liu, "Global stability of two models with incomplete treatment for tuberculosis," *Chaos, Solitons & Fractals*, vol. 43, no. 1-12, pp. 79–85, 2010. DOI:10.1016/j.chaos.2010.09.002
- [14] J. Zhang, Y. Li, and X. Zhang, "Mathematical modeling of tuberculosis data of china," *Journal of theoretical biology*, vol. 365, pp. 159–163, 2015. DOI:10.1016/j.jtbi.2014.10.019
- [15] A. Egonmwan and D. Okuonghae, "Mathematical analysis of a tuberculosis model with imperfect vaccine," *International Journal of Biomathematics*, vol. 12, no. 07, p. 1950073, 2019. DOI:10.1142/S1793524519500736
- [16] I. Syahrini, Sriwahyuni, V. Halfiani, S. M. Yuni, T. Iskandar, Rasudin, and M. Ramli, "The epidemic of tuberculosis on vaccinated population," in *Journal of Physics: Conference Series*, vol. 890, no. 1, pp. 1–6, 2017. DOI:10.1088/1742-6596/890/1/012017
- [17] M. K. Kolawole, M. O. Olayiwola, A. I. Alaje, H. O. Adekunle, and K. A. Odeyemi, "Conceptual analysis of the combined effects of vaccination, therapeutic actions, and human subjection to physical constraint in reducing the prevalence of covid-19 using the homotopy perturbation method," *Beni-Suef University Journal of Basic and Applied Sciences*, vol. 12, no. 1, pp. 1–20, 2023. DOI:10.1186/s43088-023-00343-2
- [18] A. A. Ayoade, O. J. Peter, A. I. Abioye, T. Adinum, and O. A. Uwaheren, "Application of homotopy perturbation method to an sir mumps model," *Advances in Mathematics: Scientific Journal*, vol. 9, no. 3, pp. 1329–1340, 2020. DOI:10.37418/amsj.9.3.57
- [19] M. Ibrahim, O. Peter, O. Ogwumu, and O. Akinduko, "On the homotopy analysis method for solving pstir typhoid model," *Trans. Nigerian Assoc. Math. Phys.*, vol. 4, pp. 51–56, 2017.
- [20] O. Peter and A. Awoniran, "Homotopy perturbation method for solving sir infectious disease model by incorporating vaccination," *The Pacific Journal of Science and Technology*, vol. 19, no. 1, pp. 133–140, 2018.
- [21] L. M. Erinle-Ibrahim, W. O. Lawal, O. Adebimpe, and G. R. Sontan, "A susceptible exposed infected recovered susceptible (seirs) model for the transmission of tuberculosis," *Tanzania Journal of Science*, vol. 47, no. 3, pp. 917–927, 2021. DOI: 10.4314/tjs.v47i3.4